Journal of Cerebral Blood Flow & Metabolism (2010) 30, 792–800

www.jcbfm.com

In vivo quantification of monoamine oxidase A in baboon brain: a PET study using [^{11}C]befloxatone and the multi-injection approach

Michel Bottlaender[1,3], Héric Valette[1,3], Jacques Delforge[1], Wadad Saba[1], Ilonka Guenther[1], Olivier Curet[2], Pascal George[2], Frédéric Dollé[1] and Marie-Claude Grégoire[1]

[1]*CEA, DSV, I2BM, Service Hospitalier Frédéric Joliot, Orsay, France;* [2]*Sanofi Aventis Recherche et Développement, Bagneux, France*

[^{11}C]befloxatone is a high-affinity, reversible, and selective radioligand for the *in vivo* visualization of the monoamine oxidase A (MAO-A) binding sites using positron emission tomography (PET). The multi-injection approach was used to study in baboons the interactions between the MAO-A binding sites and [^{11}C]befloxatone. The model included four compartments and seven parameters. The arterial plasma concentration, corrected for metabolites, was used as input function. The experimental protocol—three injections of labeled and/or unlabeled befloxatone—allowed the evaluation of all the model parameters from a single PET experiment. In particular, the brain regional concentrations of the MAO-A binding sites (B'_{max}) and the apparent *in vivo* befloxatone affinity (K_d) were estimated *in vivo* for the first time. A high binding site density was found in almost all the brain structures (170 ± 39 and 194 ± 26 pmol/mL in the frontal cortex and striata, respectively, $n = 5$). The cerebellum presented the lowest binding site density (66 ± 13 pmol/mL). Apparent affinity was found to be similar in all structures ($K_d V_R = 6.4 \pm 1.5$ nmol/L). This study is the first PET-based estimation of the B_{max} of an enzyme.
Journal of Cerebral Blood Flow & Metabolism (2010) **30,** 792–800; doi:10.1038/jcbfm.2009.242; published online 18 November 2009

Keywords: [^{11}C]befloxatone; baboon; *in vivo*; monoamine oxidase A; multi-injection approach; positron emission tomography

Introduction

Monoamine oxidases (MAO; EC 1.4.3.4) are flavine-containing enzymes located in the outer membrane of mitochondria. Monoamine oxidases are present in the brain (both neurons and glial cells) and in peripheral tissues. In the brain, MAOs are responsible for the metabolic inactivation of monoamine neurotransmitters and thus have a key role in the regulation of the concentration of these amines. In mammals, two isoforms of the enzyme have been identified on the basis of their biochemical properties, substrate selectivity, and gene products (Shih *et al*, 1999). These two isoforms are expressed in distinct cellular compartments within the central nervous system. Monoamine oxidase A is found primarily in catecholaminergic neurons whereas MAO-B is primary localized in serotoninergic neuron and in glial cells (Yu *et al*, 1992). According to the available literature, MAO-A could be more important than MAO-B, because it seems to be the main catabolizing enzyme of norepinephrine, serotonine, and dopamine. Dysfunction of MAO is associated with a number of neurologic disorders, including Parkinson's, Alzheimer's and Huntington's diseases, major depression, and schizophrenia (for review see Lewis *et al*, 2007). Monoamine oxidases have also been shown to be inhibited by unknown compounds contained in tobacco smoke (Van Amsterdam *et al*, 2006). Several lines of evidence indicate that the MAO-A inhibition has a key role in the nicotine addiction (Guillem *et al*, 2006; Lewis *et al*, 2007; van Amsterdam *et al*, 2006; Villegier *et al*, 2006).

Until now, the suicide substrate [^{11}C]clorgyline has been used in human positron emission tomography (PET) studies for the investigation of drugs, tobacco smoke effects, and aging (for review see Fowler *et al*, 2005). The quantification of cerebral binding of deprenyl (MAO-B) and of clorgyline (MAO-A) has been difficult because the irreversible binding of these

Correspondence: Dr M Bottlaender, CEA, DSV, I2BM, Service Hospitalier Frédéric Joliot, 4, place du Général Leclerc, F-91401 Orsay, France.
E-mail: michel.bottlaender@cea.fr
[3]These authors have contributed equally to this work.
Received 20 July 2009; revised and accepted 15 October 2009; published online 18 November 2009

substrates. This limitation has been partially overcome by the use of deuterium substitution at the α-carbon, which reduces the reaction rate so that the net blood–brain clearance can be calculated for deprenyl. But, in the case of deuterium-clorgyline, there was a decrease in the contrast of parametric images because of some nonspecific binding (Logan *et al*, 2002).

During the past decade, attention has focused on the development of reversible MAO inhibitors that are advantageous in therapeutic uses with possibly less side effects than with irreversible inhibitors (Livingston and Livingston, 1996; Wouters, 1998). Reversible and selective MAO-A inhibitors have been used as antidepressant and antianxiety drugs. Some of them have been radiolabeled and *in vivo* characterized (Ametamey *et al*, 1996; Bergström *et al*, 1997*a*; Bottlaender *et al*, 2003). *In vivo* PET studies in animals and humans have already shown the potential of [^{11}C]-harmine for imaging MAO-A (Bergström *et al*, 1997*a*, *b*; Jensen *et al*, 2006; Ginovart *et al*, 2006). [^{11}C]-harmine showed favorable kinetics and showed sensitivity to pretreatment with selective MAO-A inhibitors. (R-(−) and (S)-(+)-1-1[11C]methyl-1H-pyrrol-2-yl)-2-phenyl-2-(1-pyrrolidinyl)ethanone were also synthetized and characterized *in vivo* (Jensen *et al*, 2008). They presented two obvious advantages over harmine: a simple radiosynthesis with high yield and a slower plasma metabolism. Until now, only [^{11}C]-harmine has been used in patients (Meyer *et al*, 2006).

Befloxatone, a reversible MAO-A inhibitor, has a high affinity (2 nmol/L) and a high specificity for MAO-A sites (Curet *et al*, 1996). The ligand has been labeled with carbon-11 (Dolle *et al*, 2003) and its pharmacologic characterization was performed *in vivo* using PET in nonhuman primates (Bottlaender *et al*, 2003). [^{11}C]befloxatone attains rapidly high specific binding in brain after i.v. administration, its selective and reversible binding to MAO-A sites was also confirmed *in vivo*. Befloxatone appeared safe for its therapeutic use in humans (Rosenzweig *et al*, 1998) and therefore suitable for clinical PET (Leroy *et al*, 2009).

Quantification of brain MAO-A using PET radiotracers is based on a two-compartment model kinetic analysis. When using [^{11}C]clorgyline, the parameter $\lambda \times k_3$ (where $\lambda = k_1/k_2$, and k_3 is the catalytic activity) appears to be a more sensitive index of the inhibition of the enzyme activity than influx constant (K_i) determined with the Patlak graphical method (Lammertsma *et al*, 1991). With [^{11}C]-harmine, the kinetic modeling analysis (two-compartment model) allowed stable and reliable determination of distribution volumes (V_T) (Ginovart *et al*, 2006). However, all these methods estimate only indexes of the density of binding sites, which are only proportional to the actual binding site density or to the catalytic activity. The relation of these indexes to the density of binding sites is based on several assumptions such as equilibrium state or the K_d stability (Lammertsma *et al*, 1991; Ginovart *et al*, 2006).

The purpose of this study was to quantify the MAO-A site density in the living brain. We used the multi-injection approach that has proved to be a suitable method to estimate the binding site concentrations *in vivo* using PET: dopamine D2/D3 with fallypride and with FLB-457, benzodiazepine with flumazenil, DAT with CFT, 5-HT1A with MPPF (for review see Morris *et al*, 2009), neuronal nicotinic acetylcholine receptors with fluoro-A-85380 (Gallezot *et al*, 2008), myocardial muscarinic receptors with MQNB (Delforge *et al*, 1993). This method allows the estimations of the values of all model parameters describing the interactions between the radioligand and receptors in all brain regions. The precise parameter estimates derived from these complicated experimental protocols are necessary for proper application of drug occupancy and clinical research studies with a new radioligand. Furthermore, determination of the kinetic rate constants is important in validating simplified experimental protocols ([^{11}C]flumazenil, Delforge *et al*, 1997; [^{76}Br] and [^{11}C]FLB-457, Delforge *et al*, 2001*a*; [^{11}C]raclopride, Leriche *et al*, 2009), which are more appropriate for clinical research in humans. For the above-mentioned radioligands, it was possible to estimate B_{max} and K_d separately using a multiple-injection strategy. There are some instances where this is highly advisable: medical treatments with agonist drugs or smoking that cause receptors to change from high- to low-affinity state. In the case of MAO-A study in smokers, the estimation of B_{max} and K_d separately will allow to determine the proportion of reversible and irreversible binding of unknown compounds contained in tobacco smoke.

Simulations led to a precise knowledge of the befloxatone kinetics in all compartments. Furthermore, the these estimations has high clinical relevance as there is a close relationship between density of binding sites and activity of the MAO-A (V_{max})—the latter directly reflecting the catabolizing activity of the enzyme—as shown in human cerebral cortex and caudate nucleus (O'Carroll *et al*, 1983, 1989).

Materials and methods

Radiopharmaceutical Preparation

Befloxatone ((5R)-5-(methoxymethyl)-3-[4-[(3R)-4,4,4-trifluoro-3-hydroxybutoxy]phenyl]-2-oxazolidinone; Synthélabo, Bagneux, France) was labeled with carbon-11 ($t_{1/2}$: 20.4 mins) using [^{11}C]phosgene and the corresponding ring-opened precursor (R)-1-methoxy-3-[[4-[(3R)-4,4,4-trifluoro-3-hydroxybutoxy]phenyl]amino]-2-propanol (Dolle *et al*, 2003). Typically, 5.55 to 9.25 GBq of [^{11}C]befloxatone with a radiochemical- and chemical purity of more than 99% were routinely obtained within 25 mins of radiosynthesis (including high-pressure liquid chromatography purification) with a specific radioactivity (SA) of 11.6 to 22.7 GBq/μmol.

The Ligand-Receptor Model

The part of this model corresponding to befloxatone kinetics is derived from the usual nonequilibrium nonlinear model (Mintun *et al*, 1984; Huang *et al*, 1986). It includes four compartments (unmetabolized ligand in plasma, free ligand in the tissue, ligand specifically bound to receptor sites, and nonspecific binding; Figure 1) and seven parameters (the MAO binding site concentration (B'_{max}) and six kinetic parameters describing the kinetics between the compartments (K_1, k_2, k_5, k_6 and the apparent association and dissociation rate constants k_{on}/V_R, and k_{off})). The reaction volume V_R allows taking into account the possibility that the mean free ligand concentration in the vicinity of the receptor sites may be different from that in the entire tissue (Delforge *et al*, 1996). In the multiinjection approach, unlabeled doses of ligand are injected, and thus, the kinetics of this unlabeled ligand has to be simulated. Detailed descriptions and discussions of this procedure have been published previously (Morris *et al*, 2004; Gallezot *et al*, 2008).

Experimental Protocol

All animal use procedures were in strict accordance with the recommendations of the European Economic Community (86/609/CEE) and the French National Committee (décret 87/848) for the care and use of laboratory animals.

Five PET experiments were performed on five male *Papio anubis* (weight 13 ± 1 kg). Anesthesia was maintained with 1% isoflurane and a mixture of 66:33 nitrous oxide/oxygen, controlled by a ventilator (Ohmeda OAV 7710; Ohmeda Madison, WI, USA). The baboon's head was fixed in a head holder and positioned in the scanner gantry. A transmission scan (^{68}Ge rods, 15 mins) was recorded to correct for γ ray attenuation of subsequent emission scan.

The experimental protocol included three injections:

- a tracer dose of [^{11}C]befloxatone: 16.9 ± 5 nmol, specific activity (SA) = 16 ± 4 GBq/μmol,
- two successive coinjections of labeled and unlabeled befloxatone at 40 and 80 mins (808 ± 94 and 7719 ± 912 nmol), respectively.

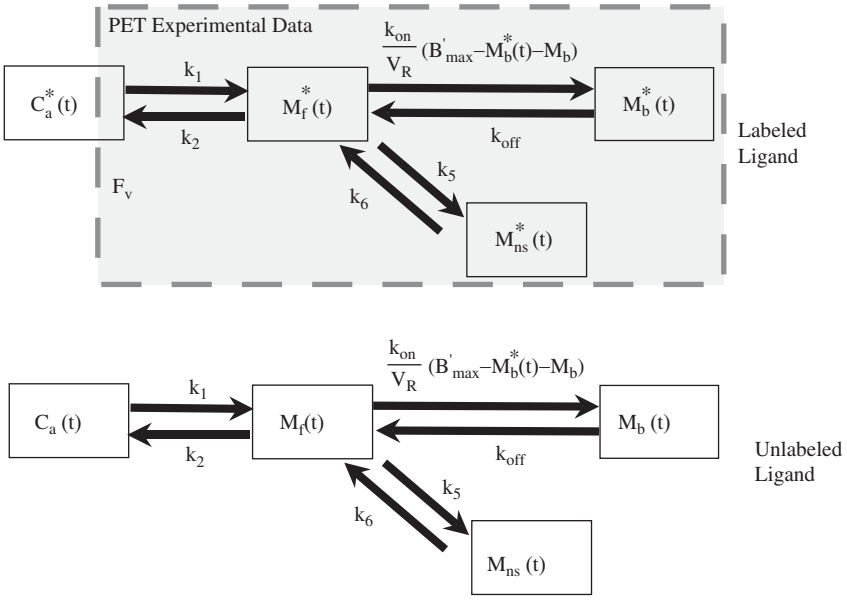

Figure 1 The plasma concentration of the unlabeled and unmetabolized ligand (denoted as $C_a(t)$) was estimated using the curve $C^*_a(t)$ corresponding to the labeled ligand. The flux of [^{11}C]befloxatone from the arterial plasma compartment to the free compartment is given by $K_1C^*_a(t)$. The free ligand can bind to an unoccupied specific receptor site, or escape back to the blood circulation with a rate constant k_2. The quantity of free labeled ligand present in 1 mL of the tissue volume is denoted by $M^*_f(t)$. However, because of the obvious heterogeneity of the tissue, this concentration can be heterogeneous in the PET volume. To take into account this heterogeneity, the concept of reaction volume, denoted by V_R, has been introduced (Delforge *et al*, 1996). By definition, the value of V_R is such that $M^*_f(t)/V_R$ is equal to the local free ligand concentration in the vicinity of the receptor sites. The specific binding is a saturable reaction that depends on the bimolecular association rate constant k_{on}, the free ligand concentration in the vicinity of the receptors sites $M^*_f(t)/V_R$, and the quantity of free receptors in 1 mL of tissue. This last quantity is equal to $B'_{max}-M^*_b(t)-M_b(t)$. B'_{max} is the total receptor site concentration available for binding. $M^*_b(t)$ and $M_b(t)$ are the quantities of receptors sites in 1 mL of tissue already occupied by the labeled and unlabeled ligands, respectively. The rate constant for the dissociation of the specifically bound ligand is denoted by k_{off}. The *in vivo* equilibrium dissociation rate constant is denoted by K_dV_R, where K_d is the ratio k_{off}/k_{on}. The simulated PET data (denoted as $M^*_{TEP}(t)$) corresponding to the PET scan performed between time t_i and t_{i+1} are given by the following equation:

$$M^*_{TEP}(t_i) = \frac{1}{t_{i+1}-t_i}\int_{t_i}^{t_{i+1}} (M^*_f(t) + M^*_b(t) + F_V C^*_b(t))\mathrm{d}t$$

where $C^*_b(t)$ is the whole blood time–concentration curve and where F_v represents the fraction of blood present in the tissue volume.

The overall duration of the experiment was 120 mins. In two experiments, the amount of [^{11}C]befloxatone produced by a single radiosynthesis was large enough to perform the three sequential injections despite of the rapid carbon-11 physical decay. However, in the three other experiments, to maintain a high count rate till the end of the scan, a second radiosynthesis was needed for the last coinjection (80 mins).

Input Function and Metabolite Studies

The input function was the arterial plasma unmetabolized [^{11}C]befloxatone. Arterial blood samples were withdrawn from the femoral artery at designated times. Blood and plasma radioactivity was measured in a γ-counter and the time–activity curves were corrected for [^{11}C] decay from the time of the first injection.

The amount of unchanged radiotracer in plasma was measured (15 samples) with high-pressure liquid chromatography. After deproteinization with acetonitrile, the samples were centrifuged and the supernatant was injected directly into the high-pressure liquid chromatography column. The column (reverse-phase Waters Bondapak C18 column (300×7.8 mm, 10 μm)) was eluted applying a gradient from 20% acetonitrile in 0.01 mol/L phosphoric acid up to 80% in 5.5 mins, up to 90% at 7.5 mins, and returned back to 20% at 7.6 mins with a total run length of 10 mins. The flow rate of the eluent was maintained at 6 mL/min. Befloxatone was eluted with a retention time of 6 mins. The data acquisition and analysis were performed using Winflow software (version 1.21; JMBS Developments, Grenoble, France).

Magnetic Resonance Imaging

An MRI examination was performed for each animal to provide detailed anatomical images. The examinations were performed with a 1.5 T SIGNA system (General Electric, Milwaukee, WI, USA) and a custom-made receive-only coil was used in proximity to the baboon's head to provide higher sensitivity. The animal was anesthetized (ketamine/xylazine, 15:1.5 mg/kg, i.m.) and positioned using a stereotaxic head holder. The imaging protocol used a T_1-weighted inversion-recovery sequence in three-dimensional mode and a 256×192 matrix over 124 slices of 1.5 mm in thickness.

PET Measurements and Data Analysis

Positron emission tomography studies were performed with a high-resolution tomograph (ECAT 953B/31; Siemens Medical Solutions, Knoxville, TN, USA), which allowed reconstruction of 31 slices every 3.3 mm with spatial and axial resolution of 5.7 and 5.0 mm, respectively. For each PET scan, a dynamic series of 48 images was acquired (3 successive and identical sets of 16 images—each set lasting 40 mins—were acquired. Each set included 4 images of 15 secs, 2 of 30 secs, 3 of 1 mins, and 7 of 5 mins). Regions of interest were drawn on magnetic resonance images in the thalamus, caudate nucleus, cerebellum, and in the frontal, occipital and temporal cortices and reported on PET images after coregistration with the corresponding magnetic resonance images using a mutual information algorithm (http://brainvisa.free.fr). Concentrations of radioactivity in the regions of interests were calculated for each frame and expressed as pmol/mL, by dividing the radioactivity by the specific radioactivity at the time of the first injection.

Results

Time–Concentration Curves

Figure 2 shows a typical time–concentration curve observed in frontal cortex (experiment 3). After the first i.v. administration of [^{11}C]befloxatone, the brain radioactivity increased rapidly. In the cortex, thalamus, striatum, the radioactivity continuously increased until 30 mins. In contrast, the cerebellar time–concentration reached a decreased peak within the first minutes and then decreased slowly (details in Bottlaender *et al*, 2003). After the first coinjection, the shape of the curves was different. In the cortex, thalamus, and striatum, the radioligand concentration peaked at 5 mins and then decreased. In the cerebellum, the peak was reached within the first minute and then decreased rapidly. The second coinjection resulted in a saturation of the MAO-A binding sites. After an early peak of radioactivity, a rapid washout was observed in all brain structures.

Model Parameter Estimates

Because of the very different shapes of the concentration curves after each of the three injections, all the parameters were estimated with good accuracy

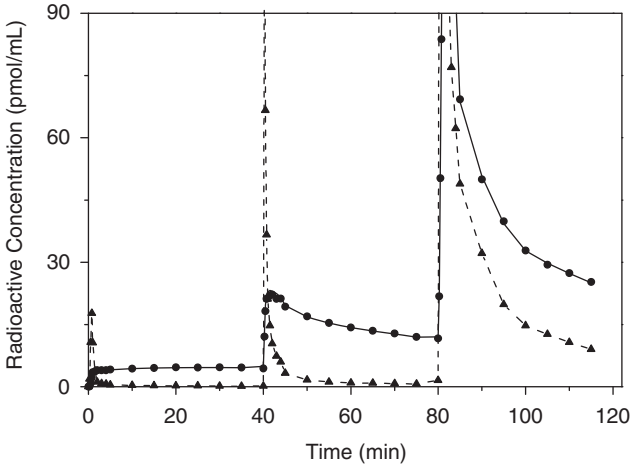

Figure 2 Plasma and PET time–activity curves obtained in frontal cortex in baboon using a multi-injection protocol. Shown is the input function (plasma unchanged befloxatone, triangle and dashed line); the experimental PET data (circles symbols); and the simulated curve obtained from the estimated model parameters (solid line). The *y* axis has been truncated at 90 pmol/mL for a better visualization of the plasma curve.

Table 1 Mean ($n = 5$ baboons), standard deviations of the model parameters identified in the seven ROIs and regional autoradiographic densities obtained in human brain[a]

Parameters	*Parameter estimates ± standard deviations*						
	Frontal Ctx	*Parietal Ctx*	*Thalamus*	*Pons*	*Caudate*	*Putamen*	*Cerebellum*
B'_{max} (pmol/mL)	199 ± 26	141 ± 27	182 ± 24	145 ± 38	194 ± 26	194 ± 30	66 ± 13
k_1 (min^{-1})	0.367 ± 0.071	0.341 ± 0.050	0.404 ± 0.071	0.402 ± 0.097	0.424 ± 0.077	0.487 ± 0.110	0.470 ± 0.102
k_2 (min^{-1})	0.495 ± 0.051	0.474 ± 0.037	0.448 ± 0.032	0.522 ± 0.075	0.513 ± 0.052	0.546 ± 0.068	0.588 ± 0.050
k_{on}/V_R mL/(pmol min)	0.006 ± 0.0017	0.008 ± 0.0027	0.005 ± 0.0013	0.005 ± 0.0010	0.006 ± 0.0019	0.005 ± 0.0015	0.006 ± 0.0019
k_{off} (min^{-1})	0.038 ± 0.012	0.045 ± 0.011	0.032 ± 0.008	0.025 ± 0.010	0.036 ± 0.013	0.032 ± 0.011	0.041 ± 0.008
k_5 (min^{-1})	0.011 ± 0.009	0.011 ± 0.008	0.010 ± 0.010	0.023 ± 0.024	0.016 ± 0.013	0.008 ± 0.007	0.011 ± 0.009
k_6 (min^{-1})	0.026 ± 0.025	0.034 ± 0.043	0.044 ± 0.057	0.057 ± 0.060	0.060 ± 0.058	0.033 ± 0.030	0.024 ± 0.022
K_dV_R (nmol/L)	6.1 ± 1.2	5.7 ± 1.1	6.8 ± 1.1	6.2 ± 2.8	6.5 ± 1.6	6.4 ± 1.4	6.9 ± 1.5
In vitro B_{max} (humans) (pmol/mL)[a]	NA	NA	NA	265	246	235	99

NA, not available.
[a]From Saura *et al* (1996).

Table 2 Individual model parameters identified in the frontal cortex during the five PET experiments

Parameters	*Parameter estimates ± standard errors*[a]					*Mean*
	Experiment 1	*Experiment 2*	*Experiment 3*	*Experiment 4*	*Experiment 5*	*± s.d.*
B'_{max} (pmol/mL)	232 ± 14	211 ± 11	163.7 ± 3.4	204.0 ± 7.2	182.8 ± 4.6	198.8 ± 26.4
k_1 (min^{-1})	0.298 ± 0.013	0.459 ± 0.024	0.348 ± 0.005	0.307 ± 0.015	0.423 ± 0.010	0.367 ± 0.071
k_2 (min^{-1})	0.425 ± 0.037	0.549 ± 0.039	0.483 ± 0.007	0.478 ± 0.023	0.542 ± 0.020	0.495 ± 0.051
k_{on}/V_R mL/(pmol min)	0.0052 ± 0.0005	0.0069 ± 0.0009	0.0061 ± 0.0002	0.0043 ± 0.0005	0.0087 ± 0.0006	0.0062 ± 0.0017
k_{off} (min^{-1})	0.029 ± 0.004	0.056 ± 0.007	0.033 ± 0.001	0.027 ± 0.003	0.044 ± 0.005	0.038 ± 0.012
k_5 (min^{-1})	0.0128 ± 0.0025	0.0043 ± 0.0010	0.0131 ± 0.0006	0.0007 ± 0.0001	0.0227 ± 0.0012	0.0107 ± 0.0086
k_6 (min^{-1})	0.053 ± 0.011	0.0003 ± 0.0001	0.036 ± 0.001	0.0003 ± 0.0002	0.043 ± 0.002	0.026 ± 0.024
K_dV_R (nmol/L)	5.6 ± 1.3	8.1 ± 2.1	5.3 ± 0.4	6.3 ± 1.5	5.07 ± 0.93	6.1 ± 1.2

[a]Standard errors estimated from the covariance matrix.

within a single experiment. Numerical values of all parameter estimates are presented in Tables 1 and 2.

In all brain structures, the quality of the fit obtained was good (Figure 2). The standard errors of the parameter estimations were low (Table 2) for all the parameters except for k_5 and k_6 where the estimation was more hazardous. But, the quality of the fit without the nonspecific binding compartment was worse according to Akaike criterion. Therefore, the complete (four-compartment) model was used.

The interindividual variability of B'_{max} was low in most of the structures (approximately 15%, Table 1). The variability was higher in the pons (25%), a fact explained by the inhomogeneity of this small structure.

The K_dV_R was found similar in all studied structures and was approximately 6 nmol/L, a value consistent with *in vitro* affinity of befloxatone: 1.3 nmol/L at 4°C (Curet *et al*, 1996).

Detailed Simulation of the Befloxatone Kinetics

With the multi-injection modeling approach, it is possible to simulate the time–concentration curves in all compartments. Figure 3 shows the simulation of the free, the specifically bound, and the nonspecifically bound labeled ligand concentrations (calculated using the input function and the model parameters in the frontal cortex of the experiment 3, Table 2).

After a tracer dose of [^{11}C]befloxatone, more than 96% of the radioactivity corresponded to labeled ligand bound to the MAO-A (Figure 3A). After 10 mins, the free ligand concentration was only 3% of the bound ligand, and the nonspecifically bound ligand concentration represented less than 1% of the bound ligand.

A similar pattern was observed after the first coinjection (Figure 3A). But, because of the large amount of unlabeled befloxatone, the distribution phase was slower. The free and nonspecifically bound fractions of labeled ligand reached a level of 5% and 1% of the bound ligand, respectively, 25 mins later.

The pattern observed after the second coinjection was different (Figure 3B). Because the MAO-A sites were saturated, the main part of the radioactivity peak corresponded to the distribution phase of the free ligand. After 20 mins, when the distribution phase was completed, the free and the bound ligand concentrations presented similar values whereas the nonspecifically bound ligand represented 60% of the bound ligand.

The unlabeled befloxatone injected at 40 mins (first coinjection) led to a partial binding site

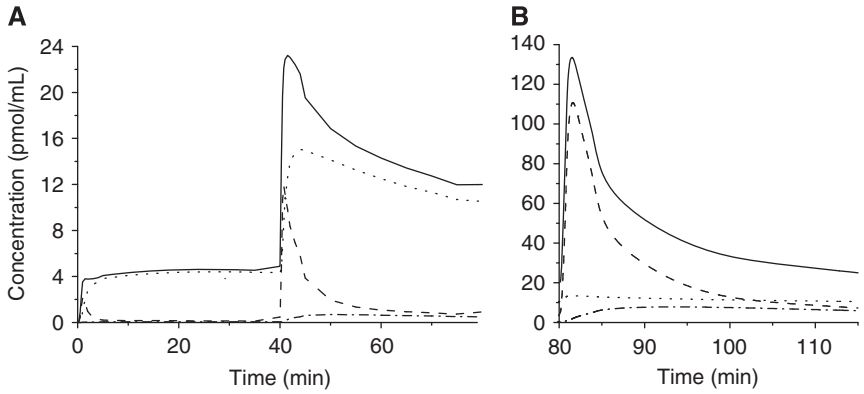

Figure 3 Simulations of the befloxatone kinetics in frontal cortex, after tracer injection and first co-injection (**A**), and after second co-injection (**B**). The befloxatone concentration is shown in all model compartments simulated using the model parameters given in Table 2 (experiment 3). Specifically bound ligand concentration: dotted line, free ligand concentration: dashed line, nonspecific binding concentration: dash-dot line, fitted PET befloxatone concentration: solid line. The left and right curves are from the same experiment, they are displayed on separates plots because of different *y* axis scales.

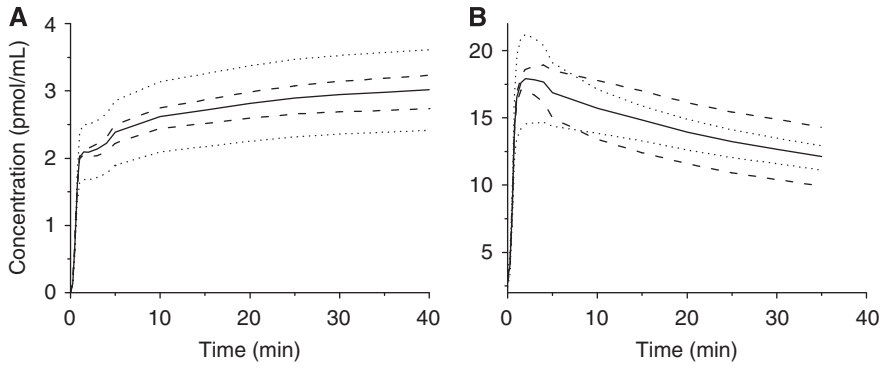

Figure 4 Simulations of changes in cerebral blood flow and receptor concentration. Solid lines show the PET time–concentration curves simulated in the frontal cortex after a tracer injection (**A**) and a low SA injection (**B**) corresponding respectively to the first and the second injections of the experiment 1. Simulations are obtained with the same model parameters, except for the receptor concentration (dashed lines) or the parameter k_1 (dotted lines), which were increased or reduced by 20%.

occupancy (approximately 75% to 65% from 60 to 80 mins), whereas the high dose of unlabeled befloxatone injected at 80 mins (second coinjection) saturated almost all binding sites (more than 95% until the end of the experiment).

Influence of the Cerebral Blood Flow and of the Binding Site Concentration on [^{11}C]Befloxatone Kinetics

A typical PET study was used to simulate PET [^{11}C]befloxatone time–concentration curves after changes in cerebral blood flow (CBF) values or MAO binding site concentrations.

After tracer injection (high SA, Figure 4A), a variation ($\pm$20%) of parameter K_1 (assumed to represent CBF) led to $\pm$20% changes in [^{11}C]befloxatone concentration and in specific binding. This was observed in all regions, as soon as 2 mins after the injection and remained constant until 40 mins. After a low SA injection (Figure 4B), the same changes in K_1 values induced a change of less than 8% of [^{11}C]befloxatone concentration.

In contrast, variations ($\pm$20%) of B'_{max} led to smaller variations in [^{11}C]befloxatone concentration (High SA, Figure 4A): +7% and −9%, respectively. However, after low SA injection, PET concentration changes were identical to B'_{max} changes: +18 and −19%, respectively (Figure 4B).

These results indicate that at high SA, PET curve is more sensitive to the CBF than to receptor density changes. Conversely, after a low SA injection where 65% to 75% of binding sites are occupied, the PET curve shape reflects the B'_{max} changes.

Study of the Equilibrium States

After a tracer injection, the equilibrium states between the three main compartments of the model were simulated (Figure 5). The equilibrium state between the plasma and the free ligand compartments (the capillary exchange equilibrium state) was estimated by the ratio of the two concentrations plasma and free ligand. As the transfer rates between the plasma and the free ligand compartments are

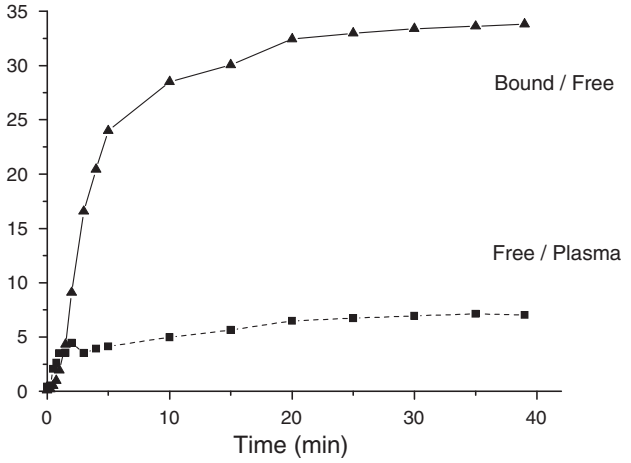

Figure 5 Study of the equilibrium states in the frontal cortex after tracer injection of [^{11}C]befloxatone (experiment 5). The dotted line (squares) represents the befloxatone concentration ratio in free over plasma compartment, the solid line (triangles) the befloxatone concentration ratio in bound over free compartment. Both curves reach a plateau at 30 mins indicating that the plasma, the free, and the bound ligand compartments are in equilibrium at this time.

linear, the equilibrium is reached when the ratio of the two concentrations is a constant, equal to k_1/k_2. The equilibrium state between the free and the bound ligand compartments is also linear, and is reached when the ratio of the two concentrations is constant, equal to $k_{on} \times B'_{max}/K_{off}$. Both ratios reached constant values after 30 mins as the consequence of a true equilibrium. Therefore, the PET protocol could be shortened to 90 mins.

Discussion

The aim of this study was to estimate the brain regional concentrations of MAO-A sites and all the ligand-binding site model parameters. This was performed during a single PET experiment by using the multi-injection modeling approach.

Experimental Protocol

Three-injection protocols have been successfully used with [^{11}C]flumazenil, [^{76}Br], or [^{11}C]FLB 457, [^{11}C]MQNB, [^{18}F]-F-A-85380 (Morris *et al*, 2009; Gallezot *et al*, 2008). In this study, the protocol included a tracer injection and two successive coinjections.

The value of k_1 was high, reflecting indicating a high extraction fraction of the tracer. Similarly, the high value of k_2 allowed rapid washout of the unbound tracer. This rapidity makes a three-injection protocol possible despite of the short period of carbon-11.

The k_{off} is six times greater than k_{on}, explaining why [^{11}C]befloxatone can be displaced relatively rapidly from its binding sites (Bottlaender *et al*, 2003). However, this displacement needs 60 mins to be complete (Bottlaender *et al*, 2003), thus, a coinjection with a partial saturating dose of befloxatone was chosen instead of a displacement with unlabeled befloxatone, for the second injection.

The third injection aimed at saturating all the MAO-A binding sites. This was achieve by a high amount of unlabeled befloxatone coinjected with [^{11}C]befloxatone to maintain a good count rate in the brain until the end of the PET experiment (120 mins).

Befloxatone appeared safe at pharmacologic doses in humans (Rosenzweig *et al*, 1998). A single dose (p.o.) of 160 mg (573 μmol) was well tolerated in volunteers, as well as repeated doses of 80 mg per day (p.o.) for 7 days. After a single oral dose of 10 mg, mean peak plasma concentration (C_{max}) was 30 ± 10 ng/mL at 2 h (t_{max}). This high plasma concentration led to an abrupt inhibition of brain MAO-A, which was, again, well tolerated. Therefore, a multi-injection protocol—using a total amount of 20 μmol i.v. befloxatone—is currently underway to quantify the MAO-A density in patients with substance abuse disorders. Administered doses of radioactivity have been adapted to humans as effective doses of [^{11}C]befloxatone were estimated to be 7.1 μSv/MBq (personal data). The PET protocol has also been shortened to avoid a second radiosynthesis. Because the equilibrium states are observed at 30 mins after injection, now the PET scan lasts 90 mins (instead of 120 mins in baboons).

Specific Binding Parameters

At tracer dose, the specific binding parameter, k_3 (given by the product $K_{on}/V_R \times B'_{max}$), is 30 times higher than k_{off} (Table 2). The parameter k_3 is three times higher than k_1 (Table 2). This indicates that the capillary exchanges are the limiting factor for the binding to MAO-sites, explaining that, at tracer dose, the PET concentration as well as the specific binding is CBF dependent (Figure 4A).

With a partial saturation, the parameter k_3 is no more linear and is given by $K_{on}/V_R \times (B'_{max} - \text{Bound})$. This situation was observed after the first coinjection where 65% to 75% of the binding sites are occupied by unlabeled befloxatone. Then, k_3 is reduced to $0.35 \pm 0.09\ \text{min}^{-1}$, a value close to that of k_1. Therefore, the [^{11}C]befloxatone binding has low sensitivity to the CBF changes (Figure 4B).

The B'_{max} values are similar in all the brain structures, with a maximum in cortical structures, striata, thalamus, and the lowest value is observed in the cerebellum. Using [^{11}C]-harmine, Ginovart *et al* (2006) also found a similar regional pattern of the distribution volumes: DV_B were 17 to 19 mL/mL in cortical structures and striata and 10.5 mL/mL in the cerebellum. In humans, Fowler (1987), using [^{11}C]clorgyline, found very close values of the influx constant (K_i from Patlak plot) in cortex, striatum thalamus, and brainstem. In studies in human brain *in vitro*, MAO-A site concentration was 1 to 3 pmol/mg of protein (Cesura *et al*, 1990; O'Carroll *et al*,

1989; Saura *et al*, 1996). Assuming a content of 100 mg proteins per mL tissue, the concentration of MAO-A can be estimated 100 to 300 pmol/mL tissue. These values are in the same range to those found in this study (Table 1).

Positron emission tomography estimations of KdVR ranged from 5.7 to 6.9 nmol depending of the region of interest (Table 1). This value is similar to that found *in vitro* by Curet *et al* (1996) using [^{3}H]befloxatone (K_d = 1.3 nmol at 4°C). This result suggests that, after saturating doses of unlabeled befloxatone used in the present PET protocol, there is no evidence of competition between endogenous substrates of MAO-A (dopamine, norepinephrine, 5HT) and befloxatone (Delforge *et al*, 2001*b*). After full inhibition of MAO-A by befloxatone in rats (befloxatone 0.75 mg/kg, p.o.), there was a clear increase in extracellular concentration of dopamine and norepinephrine measured by microdialysis (Curet *et al*, 1996). But, the *in vitro* study of the competition between [^{3}H]befloxatone and these substrates showed that they have very low affinity for MAO-A (dopamine = 0.1 mmol, norepinephrine = 1 mmol; Curet *et al*, 1996).

Nonspecific Binding

In PET studies, the nonspecific binding is often lumped together with the free ligand compartment. Neglecting the nonspecific compartment simplifies the model but is only justified if this nonspecific binding is negligible. This hypothesis was tested in our study. The quality of the fits was improved by introducing a nonspecific compartment. However, in all regions, the concentration of the nonspecific binding is very low after a tracer injection. For example, in cortical structures, k_5 is equal to $0.011 \pm 0.008\ \text{min}^{-1}$, whereas k_3 is $1.2 \pm 0.3\ \text{min}^{-1}$. At the equilibrium state, the nonspecifically bound ligand represents less than 1% of the PET concentration. Moreover, the equilibrium state between the free and the nonspecific ligand compartment is reach quickly (approximately 5 mins after a tracer injection) compared with the equilibrium states between the other compartments.

Therefore, the influence of the nonspecific binding on the PET data is minimal and, in further studies, the nonspecific compartment can be lumped together with the free compartment as the exchange is rapid even if the free and nonspecific biding are not negligible.

Conclusion

The multi-injection approach was used for the *in vivo* study of befloxatone kinetics. We have quantified for the first time *in vivo*, the density of the MAO-A binding sites in the brain. This protocol, allows the determination of all the other model parameters such as the K_d, and the kinetic rate constants. The results show that [^{11}C]befloxatone has interesting qualities for PET studies. The brain uptake is rapid and presents a high percentage of specific binding. [^{11}C]befloxatone appears to be an excellent PET ligand for pharmacologic and physiopathologic studies of the MAO-A in patients with substance abuse disorders. The present protocol has been adapted for human studies.

Disclosure/conflict of interest

The authors declare no conflict of interest.

Sanofi aventis (at the time of this study Synthelabo) simply provided the CEA (SHFJ, PET imaging center) with the following chemicals: (5R)-5-(methoxymethyl)-3-[4-[(3R)-4,4,4-trifluoro-3-hydroxybutoxy]-phenyl]-2-oxazolidinone (befloxatone, as reference compound) and (R)-1-methoxy-3-[[4-[(3R)-4,4,4-trifluoro-3-hydroxybutoxy]phenyl]amino]-2-propanol (as the precursor for the labeling with carbon-11 using [^{11}C]phosgene). No funding was received from sanofi aventis/Synthelabo for this study.

References

Ametamey SM, Beer H-F, Guenther I, Antonini A, Leenders KL, Waldmeier PC, Schubiger PA (1996) Radiosynthesis of [^{11}C]brofaromine, a potential tracer for imaging monoamine oxidase A. *Nucl Med Biol* 23:229–34

Bergström M, Westerberg G, Kihlberg T, Langström B (1997*a*) Synthesis of some ^{11}C-labelled MAO-A inhibitors and their *in vivo* uptake kinetics in rhesus monkey brain. *Nucl Med Biol* 24:381–8

Bergström M, Westerberg G, Långström B (1997*b*) ^{11}C-harmine as a tracer for monoamine oxidase A (MAO-A): *in vitro* and *in vivo* studies. *Nucl Med Biol* 24:287–93

Bottlaender M, Dolle F, Guenther I, Roumenov D, Fuseau C, Bramoulle Y, Curet O, Jegham S, Pinquier J-L, George P, Valette H (2003) Mapping the cerebral monoamine oxidase type A: positron emission tomography characterisation of the reversible selective inhibitor [^{11}C]befloxatone. *J Pharmacol Exp Ther* 305:467–73

Cesura AM, Bös M, Galva MD, Imhof R, Da Prada M (1990) Characterization of the binding of [^{3}H]Ro 41-1049 to the active site of human monoamine oxidase-A. *Mol Pharmacol* 37:358–66

Curet O, Damoiseau G, Aubin N, Sontag N, Rovei V, Jarreau F-X (1996) Befloxatone, a new reversible and selective monoamine oxidase-A inhibitor. I. Biochemical profile. *J Pharmacol Exp Ther* 277:253–64

Delforge J, Bottlaender M, Loc'h C, Dolle F, Syrota A (2001*a*) Parametric images of the extrastriatal D2 receptor density obtained using a high-affinity ligand (FLB 457) and a double-saturation method. *J Cereb Blood Flow Metab* 21:1493–503

Delforge J, Bottlaender M, Pappata S, Loc'h C, Syrota A (2001*b*) Absolute quantification by positron emission tomography of the endogenous ligand. *J Cereb Blood Flow Metab* 21:613–30

Delforge J, Le Guludec D, Syrota A, Bendriem B, Crouzel C, Slama M, Merlet P (1993) Quantification of myocardial muscarinic receptors with PET in humans. *J Nucl Med* 34:981–91

Delforge J, Spelle L, Bendriem B, Samson Y, Syrota A (1997) Parametric images of benzodiazepine receptor

concentration using a partial-saturation injection. *J Cereb Blood Flow Metab* 17:343–55

Delforge J, Syrota A, Bendriem B (1996) Concept of reaction volume in the *in vivo* ligand-receptor model. *J Nucl Med* 37:118–25

Dolle F, Valette H, Bramoulle Y, Guenther I, Fuseau C, Coulon C, Lartizien C, Jegham S, Curet O, Pinquier J-L, George P, Bottlaender M (2003) Synthesis and *in vivo* imaging properties of [^{11}C]befloxatone: a novel highly potent positron emission tomography ligand for monoamine oxidase-A. *Bioorg Med Chem Lett* 13:1771–5

Fowler JS, Logan J, Volkow ND, Wang GJ (2005) Translational neuroimaging: positron emission tomography studies of monoamine oxidase. *Mol Imaging Biol* 7:377–87

Fowler JS, MacGregor RR, Wolf AP, Arnett CD, Dewey SL, Schlyer D, Christman DR, Logan J, Smith M, Sachs H, Aquilonius SM, Bjurling P, Halldin C, Hartvig P, Leenders KL, Lundquist H, Oreland L, Stalnacke C-G, Langström B (1987) Mapping human brain monoamine oxidase A and B with ^{11}C-labeled suicide inactivators and PET. *Science* 235:481–5

Gallezot JD, Bottlaender MA, Delforge J, Valette H, Saba W, Dolle F, Coulon CM, Ottaviani MP, Hinnen F, Syrota A, Gregoire MC (2008) Quantification of cerebral nicotinic acetylcholine receptors by PET using 2-[(18)F]fluoro-A-85380 and the multiinjection approach. *J Cereb Blood Flow Metab* 28:172–89

Ginovart N, Meyer JH, Boovariwala A, Hussey D, Rabiner EA, Houle S, Wilson AA (2006) Positron emission tomography quantification of [11C]-harmine binding to monoamine oxidase-A in the human brain. *J Cereb Blood Flow Metab* 26:330–44

Guillem K, Vouillac C, Azar MR, Parsons LH, Koob GF, Cador M, Stinus L (2006) Monoamine oxidase A rather than monoamine oxidase B inhibition increases nicotine reinforcement in rats. *Eur J Neurosci* 24:3532–40

Huang SC, Barrio JR, Phelps ME (1986) Neuroreceptor assay with positron emission tomography: equilibrium versus dynamic approach. *J Cereb Blood Flow Metab* 6:515–21

Jensen SB, Di Santo R, Olsen AK, Pedersen K, Costi R, Cirilli R, Cumming P (2008) Synthesis and cerebral uptake of 1-(1-[(11)C]methyl-1H-pyrrol-2-yl)-2-phenyl-2-(1-pyrrolidinyl)ethanone, a novel tracer for positron emission tomography studies of monoamine oxidase type A. *J Med Chem* 51:1617–22

Jensen SB, Olsen AK, Pedersen K, Cumming P (2006) Effect of monoamine oxidase inhibition on amphetamine-evoked changes in dopamine receptor availability in the living pig: a dual tracer PET study with[^{11}C]harmine and [^{11}C]raclopride. *Synapse* 59:427–34

Lammertsma AA, Bench CJ, Price GW, Cremer JE, Luthra SK, Turton D, Wood ND, Frackowiak RSJ (1991) Measurement of cerebral monoamine oxidase B activity using L-[^{11}C]deprenyl and dynamic positron emission tomography. *J Cereb Blood Flow Metab* 11:545–56

Leriche L, Björklund T, Breysse N, Besret L, Grégoire MC, Carlsson T, Dollé F, Mandel RJ, Déglon N, Hantraye P, Kirik D (2009) Positron emission tomography imaging demonstrates correlation between behavioral recovery and correction of dopamine neurotransmission after gene therapy. *J Neurosci* 29:1544–53

Leroy C, Bragulat V, Berlin I, Grégoire MC, Bottlaender M, Roumenov D, Dollé F, Bourgeois S, Penttilä J, Artiges E, Martinot JL, Trichard C (2009) Cerebral monoamine oxidase A inhibition in tobacco smokers confirmed with PET and [^{11}C]befloxatone. *J Clin Psychopharmacol* 29:86–8

Lewis A, Miller JH, Lea RA (2007) Monoamine oxidase and tobacco dependence. *Neurotoxicology* 28:182–95

Livingston MG, Livingston HM (1996) Monoamine oxidase inhibitors. An update on drug interactions. *Drug Saf* 14:219–27

Logan J, Fowler JS, Ding YS, Franceschi D, Wang GJ, Volkow ND, Felder C, Alexoff D (2002) Strategy for the formation of parametric images under conditions of low injected radioactivity applied to PET studies with the irreversible monoamine oxidase A tracers [^{11}C]clorgyline and deuterium-substituted [^{11}C]clorgyline. *J Cereb Blood Flow Metab* 22:1367–76

Meyer JH, Ginovart N, Boovariwala A, Sagrati S, Hussey D, Garcia A, Young T, Praschak-Rieder N, Wilson AA, Houle S (2006) Elevated monoamine oxidase a levels in the brain: an explanation for the monoamine imbalance of major depression. *Arch Gen Psychiatry* 63:1209–16

Mintun MA, Raichle ME, Kilbourn MR, Wooten GF, Welch MJ (1984) A quantitative model for the *in vivo* assessment of drug binding sites with positron emission tomography. *Ann Neurol* 15:217–27

Morris ED, Christian BT, Yoder KK, Muzic RF (2004) Estimation of local receptor density, B′max, and other parameters via multiple-injection positron emission tomography experiments. *Methods Enzymol* 385:184–213

Morris ED, Christian BT, Yoder KK, Muzic RF (2009) Estimation of local receptor density, B′max, and other parameters via multiple-injection Positron Emission Tomography experiments. In: *Essential Bioimaging Methods—Reliable Lab Solutions* (Micheal P. Conn ed). Elsevier (in press)

O'Carroll A-M, Anderson MC, Tobbia I, Phillips JP, Tipton KF (1989) Determination of the absolute concentrations of monoamine oxidase A and B in human tissues. *Biochem Pharmacol* 38:901–5

O'Carroll A-M, Fowler CJ, Phillips JP, Tobbia I, Tipton KF (1983) The deamination of dopamine by human brain monoamine oxidase. Specificity for the two enzymes forms in seven brain regions. *Naunyn Schmiedebergs Arch Pharmacol* 322:198–202

Rosenzweig P, Patat A, Curet O, Durrieu G, Dubruc C, Zieleniuk I, Legangneux E (1998) Clinical pharmacology of befloxatone: a brief review. *J Affect Disord* 51:305–12

Saura J, Bleuel Z, Ulrich J, Mendelowitsch A, Chen K, Shih JC, Malherbe P, Da Prada M, Richards JG (1996) Molecular neuroanatomy of human monoamine oxidases A and B revealed by quantitative enzyme radioautography and *in situ* hybridization histochemistry. *Neuroscience* 70:755–74

Shih JC, Chen K, Ridgill MP (1999) Monoamine oxidase from gene to behavior. *Annu Rev Neurosci* 22:197–217

Van Amsterdam J, Talhout R, Vleeming W, Opperhuizen A (2006) Contribution of monoamine oxidase (MAO) inhibition to tobacco and alcohol addiction. *Life Sci* 79:1969–73

Villegier AS, Salomon L, Granon S, Changeux JP, Belluzzi JD, Leslie FM, Tassin JP (2006) Monoamine oxidase inhibitors allow locomotor and rewarding responses to nicotine. *Neuropsychopharmacology* 31:1704–13

Wouters J (1998) Structural aspects of monoamine oxidase and its reversible inhibition. *Curr Med Chem* 5:137–62

Yu PH, Davis BA, Boulton AA (1992) Neuronal and astroglial monoamine oxidase: pharmacological implications of specific MAO-B inhibitors. *Prog Brain Res* 94:309–15